Teleconnection Patterns in the Northern Hemisphere Simulated by IAP GCM

Xue Feng (薛 峰) and *Zeng Qingcun* (曾庆存)
Institute of Atmospheric Physics, Chinese Academy of Sciences, Beijing 100029
Received June 7, 1996; revised July 30, 1996

ABSTRACT

Based on monthly mean sea level pressure and 500 hPa height data for a 20-year period simulated by IAP 2L AGCM, teleconnection patterns in the Northern Hemisphere appearing in the model are identified and compared with observations. The results show that almost all of the observed teleconnection patterns in the Northern winter can be reproduced by the model, thus these patterns exist in the atmosphere without any external anomalies. On the other hand, the simulated teleconnection patterns are more dependent on each other than the observed, i.e., they are lack of spatial orthogonality among them, therefore, it is possible that more complex patterns will appear under the action of anomalous external factors. Besides, the simulated teleconnection patterns in summer are greatly different from those in winter, in particular, its scale in summer is much less than that in winter.

Key words: Teleconnection Patterns, Teleconnectivity, One-point correlation

I. INTRODUCTION

As recognized long ago by meteorologists, the atmospheric circulation variations in one region may result in variations in other regions, the regional variation correlation in the atmospheric circulation is called teleconnection. Early in 1930s, Walker discovered three oscillations, i.e., the South Oscillation (SO), the North Atlantic Oscillation (NAO) and the North Pacific Oscillation (NPO). After that, teleconnection has been studied by many investigators, in particular, by calculating correlations between geopotential heights, Wallace and Gutzler (Wallace and Gutzler, 1981) further revealed the existence of at least four teleconnection patterns: NAO and NPO mentioned above, a zonally symmetric seasaw between sea level pressures in polar and temperate latitudes, and the Pacific / North American pattern (PNA). These studies demonstrate that teleconnection patterns definitely exist in the atmosphere. However, do similar teleconnection patterns exist in the "climates" generated by general circulation models, and how well can the models do in simulating them, to answer these questions, by use of the monthly mean sea level pressure and 500 hPa height data for a 20-year period simulated by IAP 2L AGCM, the teleconnection patterns in the model atmosphere are identified and compared with the observed to validate the model's performance. Furthermore, the simulated results are also conducive to the studies on teleconnection patterns.

II. DATA AND METHODOLOGY

IAP 2L AGCM has been time-integrated for 25 years, the model undergoes an annual cycle without any interannual variations in sea surface temperature. The data used in this study are monthly mean sea level pressure and 500 hPa height for a 20-year period from model year 5 to model year 24, including 60 winter months (Decembers, Januaries and

Februaries) and 60 summer months (Junes, Julies and Augusts). For a sample size of 60 months, the 99% significance level corresponds to correlation coefficient. $|r_{ij}| = 0.325$, assuming that each month's anomaly pattern is independent of the others.

The method obtained by Wallace and Gutzler (hereafter referred to as WG), i.e., one-point correlation maps and teleconnectivity, is used to identify teleconnection patterns in the model. The one-point correlation maps are obtained by computing the correlation matrix R, whose elements r_{ij}a re the temporal correlation coefficients between geopotential height fluctuations at any selected grid point (denoted by the i subscript) and those at every other grid point in the hemisphere (denoted by j subscript). In each map, a region of rather strong negative correlations can be found at a distance, in some cases, several regions of negative and positive correlations combine together in an alternative manner. when the selected base grid point moves from one region to another, an ensemble of these regions with similar shapes and geographical positions is referred to as teleconnection pattern. The teleconnectivity is derived by assigning the strongest negative correlation in one-point correlation map to the base grid point. In another word, the teleconnectivity can be derived directly from the correlation matrix R by mapping the row vector T whose elements T_i are the minimum (strongest negative) values of r_{ij}, i.e.,

$$T_i = |(r_{ij}) \text{ minimum for all } j|.$$

The minus signs are omitted for the sake of convenience and T_i is termed the teleconnectivity of the ith grid point, which can be used to measure quantitatively the strength of teleconnection pattern. It is not only important to summarize the one point correlation matrix, but also conducive to the identification of teleconnection patterns.

III. TELECONNECTION PATTERNS IN THE NORTHERN WINTER

1. *Sea Level Pressure*

The study by WG shows that there are three teleconnection patterns in sea level pressure in the Northern winter, i.e., NAO, NPO and PNA pattern, which are indicative of seasaw oscillations between sea level pressures in polar and temperate latitudes. The teleconnection map (Fig.1) shows there are four centers of action, from their respective one-point correlation maps (not given), two dipole-shaped teleconnection patterns can be identified, one is located over regions from subtropical Pacific to Alaska with its strongest negative correlation of 0.75, in fact, it describes the seasaw oscillation between subtropical Pacific high and Aleutian low, this pattern obviously bears the signature of the observed PNA pattern in the position and strength of its centers, therefore, the model successfully simulates PNA pattern. Besides, there is another pattern between regions near Iceland and high latitudes of North America with its strongest negative correlation of 0.74, which is a reflection of seasaw oscillation between Icelandic low and North America cold high in the model atmosphere, but no observed pattern corresponds to this pattern (cf Fig. 7(a) in WG), so that further evidence is needed to support its existence in the real atmosphere. On the other hand, we cannot find any teleconnection patterns in the vicinity of the observed NPO and NAO.

Fig.1. The simulated teleconnectivity map of sea level pressure in the Northern winter, correlation coefficients have been multiplied by −100, arrows connect centers of strongest teleconnectivity with grid points which exhibit strongest negative correlations on their respective one-point correlation maps.

Table 1. Correlation Coefficients between Zonally Averaged Sea Level Pressures at Various Latitudes Based on 60 Winter Months Data Simulated by IAP 2L AGCM

	18°N	22°N	26°N	30°N	34°N	38°N	42°N	46°N	50°N	54°N	58°N	62°N	66°N	70°N	74°N
78°N	−0.55	−0.63	−0.65	−0.64	−0.62	−0.61	−0.55	−0.42	−0.19	0.14	0.44	0.64	0.79	0.89	0.97
74°N	−0.61	−0.68	−0.70	−0.69	−0.64	−0.60	−0.50	−0.35	−0.10	0.25	0.55	0.76	0.90	0.97	
70°N	−0.64	−0.71	−0.74	−0.73	−0.68	−0.62	−0.47	−0.28	−0.02	0.34	0.65	0.85	0.97		
66°N	−0.68	−0.75	−0.78	−0.77	−0.71	−0.61	−0.41	−0.18	0.11	0.49	0.79	0.95			
62°N	−0.70	−0.75	−0.76	−0.74	−0.66	−0.51	−0.26	0.01	0.32	0.69	0.93				
58°N	−0.67	−0.68	−0.66	−0.63	−0.53	−0.33	−0.03	0.27	0.58	0.89					
54°N	−0.54	−0.48	−0.42	−0.36	−0.24	0.01	0.32	0.62	0.87						
50°N	−0.35	−0.19	−0.08	0.02	0.15	0.40	0.69	0.91							
46°N	−0.19	0.03	0.18	0.31	0.46	0.69	0.91								
42°N	−0.03	0.24	0.43	0.58	0.73	0.91									
38°N	0.21	0.51	0.70	0.82	0.94										
34°N	0.42	0.70	0.86	0.95											
30°N	0.60	0.85	0.97												
26°N	0.76	0.95													
22°N	0.92														

From Table 1, it is obvious that the zonally averaged sea level pressures in subtropics are negatively correlated with those in high latitudes, this is in good agreement with the observed results (cf Table 1 in WG), i.e., the model simulates the anti-correlation between subtropic highs and low-pressure systems in high latitudes. According to the above analysis, it might be possible that the simulated NPO and NAO are too weak to be found in Fig.1. In fact, the one-point correlation maps at base grid points which are two centers of action in the observed NAO and NPO show that (Fig.2 and Fig.3), the simulated NAO is so weak that correlation between sea level pressures in subtropics and high latitudes cannot reach 99% significance level, thus the model fails to simulate NAO, the region with strongest negative correlation in NPO moves eastward to combine together with that in PNA pattern, i.e., the simulated NPO is located too eastward of its observed position. It should be noted, however, the discrepancies between simulation and observation are definitely related to the exclusion of interannual variations of SST from the model because NAO and NPO are almost over oceans, of course, it needs further studies to examine their detailed relationships.

2. *500 hPa Geopotential Height*

Fig.4 shows the simulated 500 hPa height teleconnectivity, in comparison with observation (cf Fig.7 in WG), four centers of action for PNA pattern and two for WP are easily found out, but it is different from observation that one center of WP (18°N,180°E) coincides with that of PNA. Based on their respective one-point correlation maps at base grid points near their centers of action (not given), arrows connecting centers of strongest teleconnectivity are determined, in the case of seasaw teleconnection patterns, arrows go in both directions. Obviously, their directions are in good agreement with observation, therefore, the model simulates the observed PNA and WP pattern. Similarly, two centers of EU pattern and three of EA can be identified, thus the model also simulates EU and EA pattern. However, the observed WA pattern cannot be found either in Fig.4 or in one-point correlation maps, i.e., the model fails to simulate WA pattern.

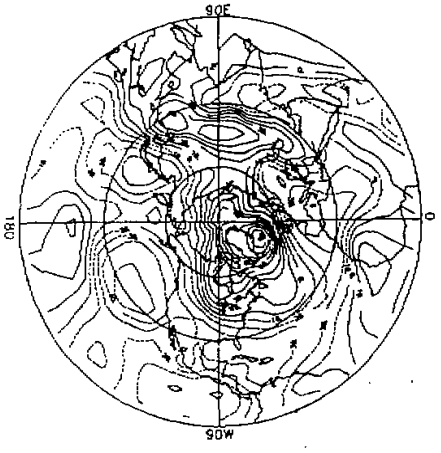

Fig.2. One-point correlation map at base grid point (60°N, 20°W), which is one of the centers of action for the observed NAO.

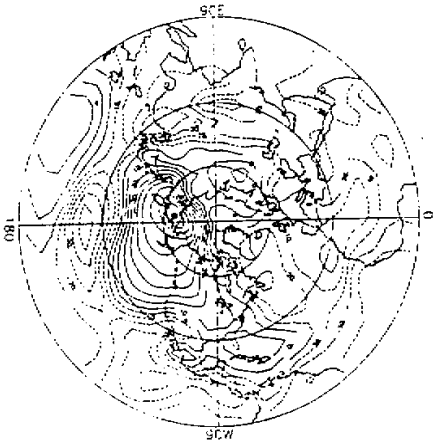

Fig.3. As in Fig.2, but at base grid point (66°N, 170°E), which is one of the centers of action for the observed NPO.

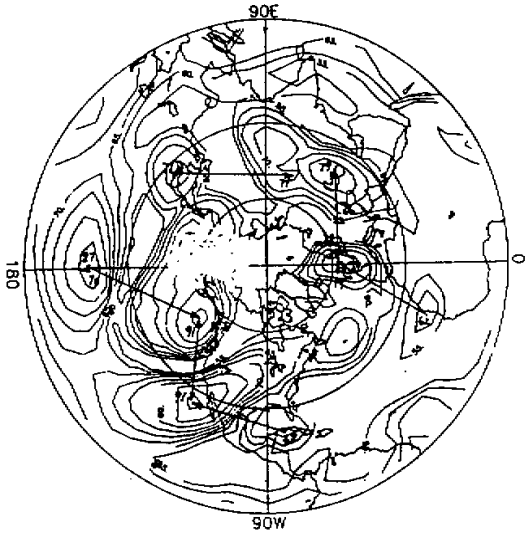

Fig.4. As in Fig.1, except for 500 hPa geopotential height.

In summary, the model simulates all of the observed teleconnection patterns except WA pattern in 500 hPa height, however, there are significant discrepancies between simulation and observation, one of centers of action (26°N, 120°W) in PNA pattern is located 30 latitudes southward of its observed position, the simulated EU pattern is lack of one center of action, and the north–south seasaw in the observed EA pattern is changed into the east–west seasaw

in simulation. Similar to the simulated WP pattern in sea level pressure, it is also positioned too eastward to separate from PNA pattern. Fig. 4 also shows that the simulated EU and EA patterns tend to combine together with each other. In fact, the simulated four teleconnection patterns make up two larger patterns , i.e, WP–PNA and EA–EU pattern, in another word, they are lack of spatial orthogonality among them, this is possibly due to that there are fewer factors in the model atmosphere such as the exclusion of air–sea interactions from the model. Furthermore, the vertical structures of teleconnection patterns are complex in both observation and simulation, but the model used in this study has only two layers in vertical directions, 500 hPa height data are obtained from interpolation between 800 hPa and 400 hPa, this may have some influences on the simulated results.

IV. TELECONNECTION PATTERNS IN THE NORTHERN SUMMER

By use of 60 summer months data, we obtain the simulated teleconnectivity map of sea level pressure in the Northern summer (Fig.5), in which two seasaw patterns are identified, one is located in East Pacific, another in West Atlantic, they are respectively termed EP and WA pattern. In the teleconnection map of 500 hPa height (Fig. 6), four patterns are identified, the first one is over regions between the Atlantic Ocean and North America with multiple centers of action, the second is in Eurasian continent with four centers of action, both the third and the fourth are seasaw patterns respectively located in East Pacific and over regions from Europe to Africa, they are termed ANA, EU, EP and EA patterns, respectively.

There have been no authoritative conclusions on teleconnection patterns in summer up to now. Huang et al. (1987), Nitta (1987) found that there exist wave trains of geopotential height emanating from the heat source region near the Philippines to North America, and these wave trains appear to be generated by intense convective activities in the Philippine Sea (Huang et al. 1987, Nitta 1987). Moreover, Huang found that teleconnection in summer is not

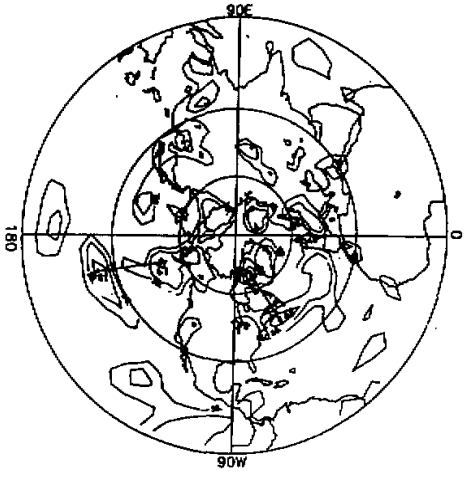

Fig.5. The simulated teleconnectivity map of sea level pressure in the Northern summer.

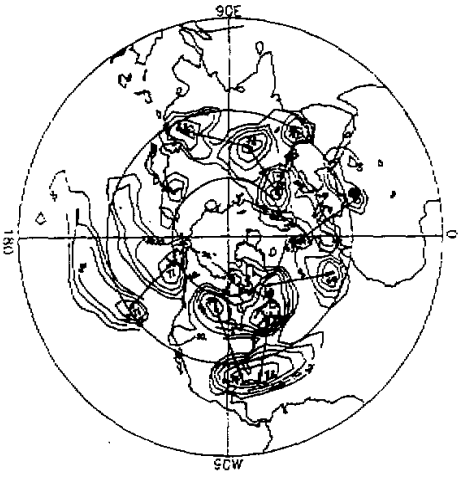

Fig.6. As in Fig.5, except for 500 hPa geopotential height.

so obvious as in winter, by using 500 hPa height deviation from zonal means for a period of 1951–1986, he identified four teleconnection patterns in the Northern summer, i.e., East Pacific / Red Sea Pattern (EPR), North Pacific / North America Pattern, Asia / Europe Pattern (AE) and Canada / Bering Sea Pattern (CB) (Huang, 1988). Besides, Yang (1992) identified four teleconnection patterns in 500 hPa height for about the same period, i.e., Asia / North America Pattern (ANA), Eurasia Pattern (EU),North-east Pacific Pattern (NEP) and North America / West Europe Pattern (AWE). In fact, there are part overlaps between the two groups of teleconnection patterns mentioned above, indicating that they are not fully indepedent each other, for instance, the geographic positions of two centers of action in NPNA Pattern identified by Huang are near those in ANA Pattern identified by Yang, but there are significant differences between them. Based on above studies, it can be concluded that teleconnection patterns also exist in the Northern summer, but they are less reproducible than in winter. While the observational uncertainty in teleconnection patterns hampers the model's evaluations, nevertheless, we can draw some inspirations from comparison between simulation and observation. It is found that the model partly reproduces the observed patterns, e.g., the positions of two centers of action in the simulated ANA Pattern are near those in ANA Pattern identified by Yang. Furthermore, comparison between the simulated patterns in summer and winter shows that their seasonal variations from winter to summer are rather large, besides different patterns, the distance between centers of action in summer is obviously less than that in winter, or the teleconnection pattern scale decreases from winter to summer. This is because that teleconnection patterns are generated by propagation of quasistationary planetary waves in the atmosphere (Hoskins and Karoly, 1981), and the scale of planetary waves in summer is less than that in winter. In addition, teleconnectivity in summer is less than that in winter on the average, showing that teleconnection in summer is not so obvious as in winter. However, it is noted that the seasonal variations in interannual variability are less than the observed (Xue and Zeng, 1996), and teleconnection is one of the phenomena in interannual variations of general atmospheric circulation. Therefore, it might

be possible that the simulated seasonal variations in teleconnection patterns are less than the observed. Finally, it is worth noting that while the above teleconnection patterns in summer do exist in the model, their existence in the real atmosphere needs further studies.

V. SUMMARY

Based on monthly mean sea level pressure and 500 hPa height including 60 winter months and 60 summer months for a 20-year period simulated by IAP 2L AGCM, teleconnection patterns in the model are identified and compared with observation, the main results are summarized as follows:

(1) The model simulates almost all of the observed teleconnection patterns in the Northern winter, showing that these patterns do exist in the atmosphere without any external anomalies. However, the simulated patterns are more dependent upon each other as compared with the observed, i.e., they are lack of spatial orthogonality among them, therefore, more complex patterns might appear under the action of the external factors. Besides, the model captures their vertical structure, i.e., they have more complex structure in 500 hPa height than in sea level pressure.

(2) The model partly reproduces the observed patterns in summer. By comparison, it is found that the teleconnection pattern scale in summer is obviously less than that in winter. However, the observational uncertainty hampers the model's evaluations, therefore, further studies are needed to examine the existence of the above patterns in the real atmosphere.

REFERENCES

Hoskins, B.J. and D. Karoly (1981), The steady, linear response of a spherical atmosphere to the thermal and orographic forcing, *J. Atmos. Sci.*, **38**: 1179-1196.

Huang, J.-P. (1988), Observational and theoretical studies on monthly mean atmospheric circulation anomaly and its numerical simulation, Ph.D. dissertation, Lanzhou University, pp 226.

Huang, R.-H. et al. (1987), Influence of the heat source anomaly over the western tropical Pacific on the subtropic high over East Asia, *Proceedings of the International Conference of the General Circulation of East Asia*, Chengdu, 40-45.

Nitta, T. (1987), Convective activities in the tropical western Pacific and their impact on the Northern Hemisphere summer circulation, *J. Meteor. Soc. Japan*, **65**: 373-390.

Wallace, J.M. and D.S. Gutzler (1981), Teleconnections in the geopotential height field during the Northern Hemisphere winter, *Mon. Wea. Rev.*, **109**: 784-812.

Xue, F. and Q.-C. Zeng (1996), Numerical simulation of interannual variability in the atmosphere, *Chinese J. Atmos. Sci.*, in press.

Xue, F. (1992), The statistical analysis of climate simulation and validation of IAP GCM, Ph.D. dissertation, Institute of Atmospheric Physics, Chinese Academy of Sciences, pp 173.

Yang,X.-Q. (1992), Observational study of teleconnections in the geopotential height during the Northern Hemisphere summer, *Chinese J. Atmos. Sci.*, **16**: 513-521.